New Strategy for Chromium Substitution and Crystal Morphology Control—Synthesis and Characteristics of CrAPO-5

Jan Kornatowski,*,† Gabriela Zadrozna,†,‡ Michal Rozwadowski,§ Bodo Zibrowius,|| Frank Marlow,|| and Johannes A. Lercher†

Institute of Chemical Technology II, University of Technology, 85747 München, Germany, Institute of Organic Chemistry and Technology, Cracow University of Technology, 31-155 Krakow, Poland, Faculty of Chemistry, Nicholas Copernicus University, 87-100 Torun, Poland, and Max-Planck-Institut für Kohlenforschung, 45470 Mülheim a. d. Ruhr, Germany

Received October 5, 2000. Revised Manuscript Received August 28, 2001

Additional component(s) introduced into the reaction gel allow for a stable framework substitution of Cr in significant amounts. Appropriate component(s) and metal compounds, especially those of Al, are primary factors determining the substitution. The products of the system {triethylamine−acetate ions−Cr^{3+} ions} have been characterized in more detail and compared with those from other synthesis procedures. The Cr heteroatoms are 4-fold bonded to the framework and their coordination is complemented by two ligands from the pores (water molecules in the calcined form) to give the favored octahedral-like coordination. The coordination can be changed reproducibly from 6 to 4 by heating the crystals over 550 K (dehydration) and vice versa by cooling (hydration). The framework Cr(III) cannot be oxidized and causes no framework charge. The reaction conditions, differing from those in the classical syntheses, enable the control of the crystal morphology. The crystals can be grown as flat hexagonal pellets of a perfect morphology with high crystallinity and sorption properties.

Introduction

One of the fascinating questions for isomorphous substitution of heterometals into molecular sieves is why some metals can easily be introduced into the framework while many others seem to be impossible to incorporate. The most important factors for substitution are ionic radius, ionic charge, affinity to the formation of tetrahedral coordination with oxygen, and difference in acidic/basic properties in relation to the main framework atoms.[1,2] Metals forming several ions of various valences, amphoteric properties, coordination states, or structures, among them Cr, belong to the group difficult for substitution. Despite this, progress in the substitution of such metals is observed and new possibilities are emerging, for example, (i) framework vanadium able to change reproducibly its valence and/or coordination[3] and (ii) chromium forming a distorted, partially "extra-framework" octahedral coordination.[4,5] Introduction of such metals into the framework appears mainly to be related to appropriate conditions during the synthesis.[3−5]

Substitution of Cr into $AlPO_4$-5 was claimed for the first time by Flanigen et al.[6] Xu, Maddox, and Thomas[7] synthesized CrAPO-5 using the fluoride method but did not show proof for the framework incorporation of Cr. From extensive spectroscopic studies of Cr in $AlPO_4$-5 and various silicates, Weckhuysen and Schoonheydt[8,9] concluded generally that Cr^{3+} cannot occupy framework positions mainly because of a strong preference for octahedral coordination. In a number of papers on catalytic activity of CrAPO-5 materials, Sheldon and coworkers[10−13] postulated framework incorporation of Cr^{3+} and Cr^{6+} in both tetrahedral and octahedral coordinations without, however, experimental evidence. They later showed[14] that the calcined materials evolved Cr^{6+} species during catalytic reactions. Radaev et al.[15] re-

* To whom correspondence should be addressed.
† University of Technology.
‡ Cracow University of Technology.
§ Nicholas Copernicus University.
|| Max-Planck-Institut für Kohlenforschung.

(1) Barrer, R. M. *Zeolites and Clay Minerals as Sorbents and Molecular Sieves*; Academic Press: London, 1987.
(2) Bennett, J. M.; Cohen, J. P.; Flanigen, E. M.; Pluth J. J.; Smith, J. V. *Am. Chem. Soc., Symp. Ser.* **1983**, *218*, 109.
(3) (a) Kornatowski, J.; Wichterlova, B.; Rozwadowski, M.; Baur, W. H. *Stud. Surf. Sci. Catal.* **1994**, *84*, 117; (b) Kornatowski, J.; Wichterlová, B.; Jirkovský, J.; Löffler, E.; Pilz, W. *J. Chem. Soc., Faraday Trans.* **1996**, *92*, 1067. (c) Kornatowski, J.; Sychev, M.; Baur, W. H.; Finger, G. *Collect. Czech. Chem. Commun.* **1992**, *57*, 767.
(4) Kornatowski, J.; Zadrozna, G. In *Proceedings 12th International Zeolite Conference, Baltimore, July 1998*; Treacy, M. M. J., Marcus, B. K., Bisher, M. E., Higgins, J. B., Eds.; Materials Research Society, Warrendale, PA, 1999; Vol. 3, p 1577.
(5) Kornatowski, J.; Zadrozna, G.; Wloch, J.; Rozwadowski, M. *Langmuir* **1999**, *15*, 5863.
(6) Flanigen, E. M.; Lok, B. M. T.; Patton, R. L.; Wilson, S. T. U.S. Patent 4,759,919, 1988.
(7) Xu, Y.; Maddox, P. J.; Thomas, J. M. *Polyhedron* **1989**, *8*, 819.
(8) Weckhuysen, B. M.; Schoonheydt, R. A. *Zeolites* **1994**, *14*, 360.
(9) Weckhuysen, B. M.; Schoonheydt, R. A. *Stud. Surf. Sci. Catal.* **1994**, *84*, 965.
(10) Chen, J. D.; Dakka, J.; Neeleman, E.; Sheldon, R. A. *J. Chem. Soc., Chem. Commun.* **1993**, 1379.
(11) Sheldon, R. A.; Chen, J. D.; Dakka, J.; Neeleman, E. *Stud. Surf. Sci. Catal.* **1994**, *83*, 407.
(12) Chen, J. D.; Haanepen, M. J.; van Hooff, J. H. C.; Sheldon, R. A. *Stud. Surf. Sci. Catal.* **1994**, *84*, 973.
(13) Lempers, H. E. B.; Chen, J. D.; Sheldon, R. A. *Stud. Surf. Sci. Catal.* **1995**, *94*, 705.
(14) Lempers, H. E. B.; Sheldon, R. A. *Stud. Surf. Sci. Catal.* **1997**, *105*, 1061.

10.1021/cm0011864 CCC: $20.00
Published on Web 12/17/2001

ported on the synthesis of large CrAPO-5 crystals using the fluoride method and on crystal structure refinement. They concluded that Cr rather occurs as an extra-framework species. The same materials investigated by Thiele et al.[16] with UV−Vis spectroscopy revealed only an octahedral coordination of Cr and a partial collapse of structure under calcination. Zhu et al.[17] concluded from the EPR measurements of CrAPSO-11 that Cr^{3+} retained in the as-prepared crystals is oxidized, during calcination, to Cr(V), which remains stable and can change its coordination from tetrahedral to square pyramidal and vice versa upon hydration−dehydration treatments. After our first report[4] on stable framework substitution of Cr^{3+} into $AlPO_4$-5, Zhu and Kevan[18] published EPR studies on CrAPSO-5. They proposed that small amounts of Cr (0.043 mol %) substitute for P(V), as Cr^{3+} in the as-prepared crystals and as Cr(V) after calcination. Miyake et al.[19] claimed incorporation of small Cr amounts into the framework of CrAPO-5 grown with tripropylamine but showed no evidence.

Trivalent Cr^{3+} is an exceptional substituent, as the resulting aluminophosphate molecular sieves do not reveal a framework charge.[4,5,7] We have already reported on these unique CrAPO-5 materials: the relationship between the sorption properties and theoretical considerations,[5] EPR of Cr in the substituted and not substituted materials,[20] and the catalytic behavior in conversion of alcohols[21] (the materials are rather not favorable redox catalysts because of the stability of Cr^{3+}). The perfect structure and morphology make the crystals promising matrixes for optics and lasers.

Our new synthesis strategy involves introduction of additional components into the synthesis gel. We call the components "co-templates" and use this term not in the traditional meaning limited to the crystallographic structure of the framework, but in a broader one, comprising all aspects of the product: framework structure, chemical composition, and crystal morphology. Thus, the co-templates are the compounds necessary for the synthesis of CrAPO-5 materials, though they are not necessary for the formation of an AFI-type structure. The term is also used to stress the active role of these components in the syntheses, as this role could not be clear from the other terms, for example, "additive".

In this work, we report on a synthesis yielding CrAPO-5 richer in framework Cr^{3+} ions and show the differences between such materials and those prepared without our new strategy. A special focus is on the role of co-templates and the synergetic effects between these additional components and metal compounds. The characteristics are shown with reference to the synthesis conditions. We report here in details on one system, with acetate ions as co-template. The co-template(s) have been introduced to investigate both the possibility of substitution and the affinity of the system to incorporation of Cr^{3+} ions. The use of other favorable co-templates is reported separately.[22] Similar co-templating effects have also been observed[23] for materials other than CrAPO-5. Thus, all these results, though not all reported in the present paper, allow us to claim a new synthesis strategy of a more general significance.

Experimental Section

Synthesis. The new synthesis strategy has been derived from our method for growing large crystals of aluminophosphate molecular sieves,[24] already successfully applied by other authors (e.g., refs 15, 16, 25, and 26). The reaction gels had the following molar ratios of components as oxides: *a*:1.00:*b*: 1.55:270:0.1 for Al_2O_3:P_2O_5:Cr_2O_3:TEA:H_2O:X, where $a + b = 1.00$ and $b = 0.05-0.2$. TEA (triethylamine) was the standard template. X represented compounds tested as potential co-templates: alcohols, organic acids, inorganic acids and salts of alkaline metals and ammonia, other amines and quaternary ammonium salts, buffers, and media increasing the viscosity/density of reaction gels (glycol, glycerol, starch, etc).

The tested Al sources were crystalline hydroxides Pural SB and Catapal B (73.6% Al_2O_3) of pseudoboehmite structure, pseudoboehmite-like Al oxide hydrate sol,[24] Al sulfate, acetate, isopropoxide, and phosphate salts (all Merck) and amorphous Al hydroxide sols/gels (Giulini Chemie). Cr was used in the form of $Cr(NO_3)_3 \cdot 9H_2O$, $CrCl_3 \cdot 6H_2O$, or Cr acetate (all Aldrich).

The initial mixture (A) was formed by sequential dissolving/dispensing of an Al compound, a Cr salt, and co-template(s) in water under vigorous stirring.[24] The mixture (B) was formed by reacting H_3PO_4 (85 wt %, Merck) diluted ≈1:1 in water with triethylamine (Merck), which was added when stirred and cooled. After (B) was added to (A), the mixture was homogenized by stirring at room temperature, then placed in PTFE-lined autoclaves, and heated at 463 K for 16−72 h. Comparative syntheses were made following the classical[2] method (reaction gel prepared by successive addition of all components to one mixture) and using chromate salts.

All products were decanted in water until free of the remains of the unreacted gel, then filtered, washed, dried at 380 K overnight, and calcined under air at 773 K for 2 days.

Characterization Methods. XRD patterns were recorded (Siemens D 5000, Cu Kα) for unground samples equilibrated in open air for at least 24 h after the preceding thermal treatments (drying or calcination). Chemical analysis was done with the inductive coupled plasma (ICP) method (Spectroflame D). The morphology of the crystals, their dimensions, and the crystal size distribution were examined using scanning electron microscopy (SEM). The optical properties of the crystals were estimated with polarization light microscopy. Diffuse reflectance UV−Vis spectra were recorded for unground samples (Lambda 7, Perkin-Elmer). The spectra at an elevated temperature were recorded for the samples placed in a metallic sample holder and preheated ex situ to ≈570 K. The X-band EPR spectra (9.66 GHz) were measured at room temperature (Bruker ER 200/ESP 3220). The ^{27}Al and ^{31}P MAS NMR spectra, measured for the samples 2, 5, 11, and 15 (Table 1), were recorded at resonance frequencies of 78.2 and 121.5 MHz, respectively, and spinning rates of at least 5 kHz (Bruker MSL

(15) Radaev, S. F.; Joswig, W.; Baur, W. H. *J. Mater. Chem.* **1996**, *6*, 1413.
(16) Thiele, S.; Hoffmann, K.; Vetter, R.; Marlow, F.; Radaev, S. *Zeolites* **1997**, *19*, 190.
(17) Zhu, Z.; Wasowicz, T.; Kevan, L. *J. Phys. Chem. B* **1997**, *101*, 10763.
(18) Zhu, Z.; Kevan, L. *Phys. Chem. Chem. Phys.* **1999**, *1*, 199.
(19) Miyake, M.; Uehara, H.; Suzuki, H.; Yao, Z.; Matsuda, M.; Sato, M. *Microporous Mesoporous Mater.* **1999**, *32*, 45.
(20) Padlyak, B.; Kornatowski, J.; Zadrozna, G.; Rozwadowski, M.; Gutsze, A. *J. Phys. Chem.* **2000**, *104*, 11837.
(21) Zadrozna, G.; Sauvage, E.; Kornatowski, J., to be published.
(22) Kornatowski, J.; Zadrozna, G.; Lercher, J. A.; Rozwadowski, M. In *Proceedings of the 13th International Zeolite Conference, Montpellier, France, 2001*; Studies in Surface Science and Catalysis 135; Elsevier: Amsterdam, 2001
(23) Kornatowski, J.; Zadrozna, G.; Lercher, J. A., to be published.
(24) (a) Kornatowski, J.; Finger, G. *Bull. Soc. Chim. Belg.* **1990**, *99*, 857. (b) Finger, G.; Richter-Mendau, J.; Bulow, M.; Kornatowski, J. *Zeolites* **1991**, *11*, 443. (c) Kornatowski, J.; Rozwadowski, M.; Finger, G. Polish Patents 166147, 166149, 166162, 166505, 1995.
(25) Demuth, D.; Stucky, G. D.; Unger, K. K.; Schüth, F. *Microporous Mater.* **1995**, *3*, 473.
(26) Kodaira, T.; Miyazawa, K.; Ikeda, T.; Kiyozumi, Y. *Microporous Mesoporous Mater.* **1999**, *29*, 329.

Table 1. Characteristics of the Crystals in Various CrAPO-5 Samples[a]

no.	Al species used for the synthesis	crystal dimensions, $l \times d^{+}$ (μm)	colors of the calcined crystals: at RT, hydrated	colors of the calcined crystals: above 550 K, dehydrated	N_2 volume in micropores[b]: gaseous (cm^3/g)	N_2 volume in micropores[b]: liquid (cm^3/g)	Cr/P in gel	analytical (ICP) content (mol %): P	Al	Cr	u.c./Cr and (Cr/u.c.)
1[@]	$Al(OH)_3$ sol (PB)*	100−130 × 30−40	yellow-green	violet	75	0.0977	0.05	49.4	50.0	0.59	7.1 (0.14)
2	$Al(OH)_3$ sol (PB)*	10−20 × 40−50	yellow-green	violet	69	0.0926	0.10	49.7	48.1	2.16	1.9 (0.53)
3	Pural SB	10−20 × 10−50	yellow-green	violet	87	0.1229	0.065	49.8	48.8	1.40	2.9 (0.34)
4	Pural SB	50−60 × 50−60	yellow-green	violet	86	0.1219	0.05	50.0	48.6	1.35	3.0 (0.33)
5	Pural SB	10−40 × 30−50	yellow-green	violet	76	0.1018	0.05	49.8	48.9	1.31	3.1 (0.32)
6[@]	Pural SB	10−50 × 10−50	yellow-green	violet	76	0.1076	0.05	50.1	48.8	1.07	3.8 (0.26)
7	Pural SB	5−50 × 5−60	yellow-green	violet	76	0.1089	0.05	49.8	49.3	0.94	4.3 (0.23)
8[?]	Pural SB	10−20 × 30−70	yellow-green	violet	85	0.1195	0.075	50.1	49.0	0.84	5.0 (0.20)
9[@]	Pural SB	80−100 × 40−50 10−20 × 30−50	yellow-green	violet	79	0.1131	0.05	50.1	49.1	0.74	5.6 (0.18)
10[?]	Pural SB	50−120 × 10−40 20−70 × 50−60	yellow-green	violet	65	0.0918	0.056	50.2	49.1	0.76	5.6 (0.18)
11[?]	Pural SB	50−70 × 50−70 10−20 × 50−60	yellow-green	violet	94	0.1292	0.025	50.0	49.5	0.42	10.0 (0.10)
12[@]	Pural SB	100−300 × 10−40	greenish-gray	greenish-gray	79[⊗]	0.0245	0.05	41.8	57.7	0.45	9.1 (0.11)
13[?]	Catapal B	60−120 × 10−50	yellow	greenish-gray	70[⊗]	0.0711	0.075	42.3	55.1	2.57	1.6 (0.63)
14[@,T]	Catapal B	150−200 × 20−40	yellowish-gray	greenish-gray	65[⊗]	0.0678	0.05	46.4	53.1	0.45	9.1 (0.11)
15[H]	$Al(OH)_3$ sol (am.)	200−400 × 50−60	gray	gray	15	0.0212	0.10	48.7	50.5	0.74	5.6 (0.18)
16	$Al(OH)_3$ sol (am.)	300−350 × 10−50	gray	gray	7	0.0086	0.10	49.9	49.8	0.33	12.5 (0.08)
17[@,H]	$Al(OH)_3$ sol (am.)	400 × 30−50	gray	gray	7	0.0099	0.05	50.2	49.5	0.31	14.3 (0.07)
18[@]	$Al(OH)_3$ sol (am.)	120−300 × 10−50	gray	gray	10	0.0153	0.05	49.9	49.9	0.24	16.7 (0.06)

[a] No. 1−11: samples of high sorption capacities (HS). No. 12−14: comparative syntheses with chromate salt (12) and with classical method[2] (13,14). No. 15−18: samples of low sorption capacities (LS). Symbols: (@) no acetate in the gel. (?) $Al_2O_3 = 1.00$ in the gel [$(a + b) > 1$, cf. Experimental Section]. (H) 0.03 M H_2SO_4 added to the gel to lower pH. (T) TEA = 1.00 in the gel (classical composition[2]). (+) *l*, length; *d*, width of the crystals. (*) PB, pseudoboehmite-like. (⊗) Additional significant amount of meso- or macropores. [b] Values at $p/p_s = 0.80$. Volume of gas (STP) multiplied by 0.0015644 gives the liquid N_2 volume. (am.) = amorphous.

300). All the spectra were obtained by single-pulse excitation (0.75 μs (π/12) for ^{27}Al and 3.0 μs (π/2) for ^{31}P) with appropriate repetition times (1 s for ^{27}Al and 15−30 s for ^{31}P). High-power proton decoupling was applied for the ^{31}P MAS NMR spectra of the as-synthesized samples. Fluorescence spectra and photographs were taken with a UV/Vis microscope photometer MPV-SP (Leica) using a Hg lamp to excite the fluorescence at 365 nm. Sorption isotherms for water and benzene were determined in a vacuum device with a McBain quartz spring balance and an MKS Baratron gauge at 298.2 K. The samples were activated before the measurements by heating in situ to 800 K under vacuum until constant mass was attained (at least 8 h). Each point of the isotherms was recorded after the equilibrium state was achieved. Pore volumes were determined from nitrogen adsorption at 77 K using the ASAP 2010 instrument (Micromeritics). The thermogravimetric analyses (TG, DTG, and DSC curves) were recorded at a heating rate of 2 K/min (Netzsch STA 409C). The tests for leaching Cr from the crystals were performed by stirring CrAPO-5 samples in 0.5 and 1 M acetic acid solutions at room temperature for up to 15 days and analyzing both the crystals and the solution. The thermal stability was checked by several repeated cycles of calcination at 773 K and cooling to room temperature under air. The ion exchange properties were tested by treating the CrAPO-5 crystals with 0.1 and 1 M NaCl solutions under stirring at room temperature for 48 h (repeated three times) and analyzing the solutions for Cr.

Results and Discussion

Synthesis Procedure and the Significance of the Compounds Used. The investigations of the synthesis procedure included three main points: (i) induction of co-templating effects by the use of additional components in the reaction gel, (ii) exploration of the significance of various Al compounds, and (iii) probing the influence of Cr compounds on the synthesis and products.

Of the large group of tested co-templates (Experimental Section), organic acids displayed the most favorable influence on the products and the second group was

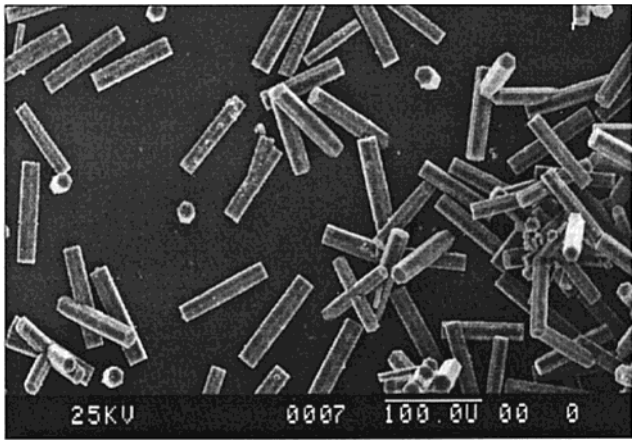

Figure 1. SEM micrographs of CrAPO-5 (sample 18) with extra-framework Cr (gray after calcination). The elongated hexagonal prisms indicate no effect of Cr on morphology.

aliphatic alcohols. In particular, the syntheses resulted in more pure crystalline phases, a higher yield, and a better morphology of the crystals than those without or with the other co-templates. Therefore, we focused on the group of acids and report here on the chosen example system containing acetate ions as the co-templating and buffering agent that could be introduced as acetic acid or as a metal acetate.

The crystalline phases were formed in all batches (Figures 1 and 2) with the yield typical for the procedure,[24] that is, 60−100% depending on the gel composition, amount(s) of co-template(s), crystallization period, and the Al compound used. After the products were decanted in water, the remains of amorphous, unreacted gel and/or crystalline byproducts were observed only occasionally and in small amounts (Figures 1 and 2). The byproducts occurred mostly as aggregates with significantly smaller primary crystallite size than

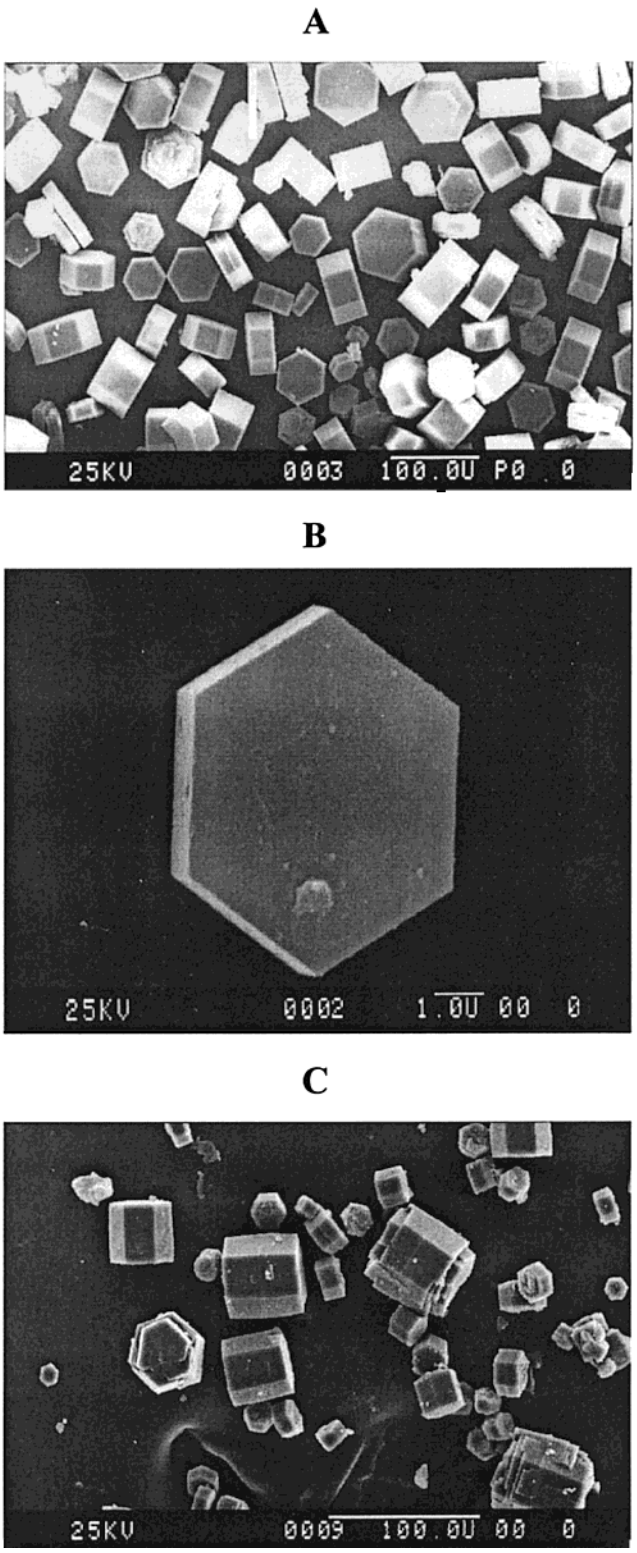

Figure 2. SEM micrographs of CrAPO-5 samples No. 8 (A) and 10 (B) (Table 1) with the stably incorporated Cr^{3+} ions (green or yellow-green after calcination) showing the characteristic morphology of flat hexagonal pellets. The low content of Cr exerts a weaker influence on morphology (micrograph C, sample 11).

CrAPO-5. The reaction gel composition influenced mainly the yield and rate of crystallization as well as the amount of incorporated Cr to some extent.

The reaction gels with the amorphous Al compounds changed their pH value immediately after the initial

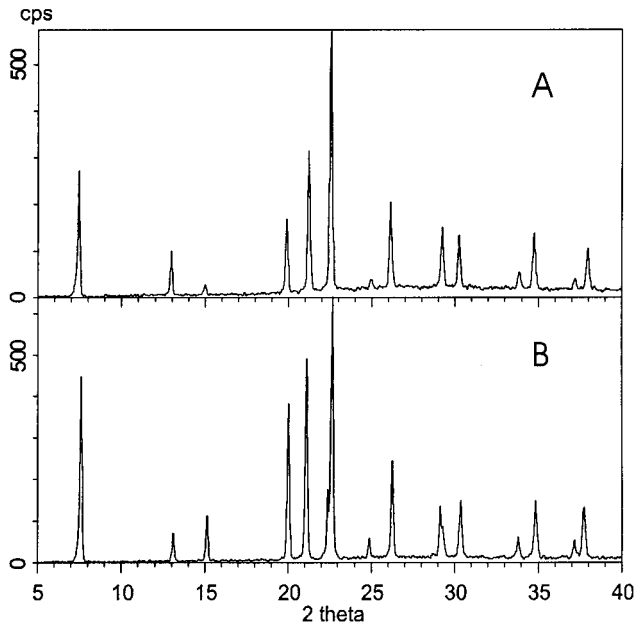

Figure 3. XRD patterns of CrAPO-5 sample of high sorption capacities (HS sample 2, Table 1): (A) calcined; (B) as-prepared.

mixtures were combined and ΔpH reached 2 and more after 20 min of stirring. The crystalline Al compounds caused the ΔpH to be lower than 0.5, even after several hours of stirring. The pH values after the crystallization were also higher by about 2 for the amorphous Al compounds. Thus, the two types of Al compounds react in distinct ways, yielding various products.

The Cr content of the samples (ICP) varied from 0.5 to 0.06 Cr per u.c., that is, 2 to 16.5 u.c. per 1 Cr atom (Table 1) and did not directly depend on the amount used in the synthesis gel. It differed for crystals synthesized from apparently similar gels with the same amount of Cr by a factor of up to 3, even when the same Al compounds were used (Table 1), because of the ratios of particular components and especially the amount of co-template and type of Cr^{3+} compound.

The method of the gel preparation apparently had a lower influence on the quality of CrAPO-5 (Table 1, samples 13 and 14). Our method allowed, however, for introduction of higher amounts of Cr into the framework positions than the classical one.[2] The comparative syntheses (classical method[2]) with and without the co-templates also yielded crystalline phases differing, however, in the crystal morphology (see below) and having a lower phase purity. Chromate compounds yielded greenish-gray crystals containing very low amounts of Cr^{3+}, probably formed by partial reduction of chromates by organic templates during synthesis (Table 1, sample 12).

XRD Investigation. The XRD patterns of all the as-prepared products (Figures 3 and 4) indicated the AFI structure type. The strong differences in the relative intensities of the lines indicated a clear division of the samples into two groups. The XRD patterns of the samples from the pseudoboehmite(-like) Al compounds were very similar to that commonly known for the AFI

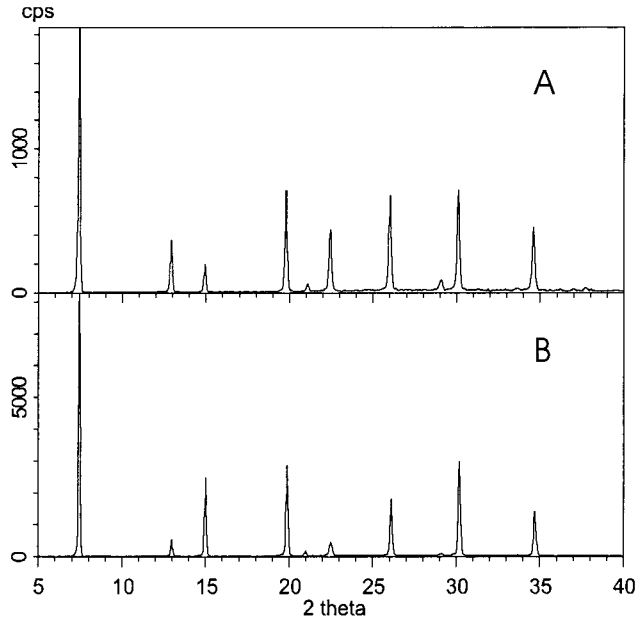

Figure 4. XRD patterns of CrAPO-5 sample of low sorption capacities (LS sample 15, Table 1): (A) calcined; (B) as-prepared.

structure type[27] and had the most intense (211) or (210) line at about 22.3° or 19.7° 2θ, respectively (Figure 3). The patterns of the calcined samples remained unchanged (Figure 3), indicating a good thermal stability of the materials.

For the samples synthesized from the amorphous Al compounds, the patterns showed an extremely intense (100) line at about 7.4° 2θ (Figure 4). After calcination, the patterns decreased in intensity by a factor of 4−10 (Figure 4). These unusually high differences were reproducibly recorded for all the samples of that group. Similar high intensities of the XRD patterns for the as-synthesized CrAPO-5 materials and a very strong decrease in the intensities after calcination were already reported by Radaev et al.[15] (not incorporated Cr, cf. Introduction). We observed additionally that the calcined samples of this group contain some amorphous material (XRD) and a significant amount of meso- and macropores (cf. Sorption section). Considering the relatively high amounts of chromium retained in the crystals (Table 1), one could assume that Cr might be partially substituted into the framework during the synthesis in unstable positions either for phosphorus as Cr^{5+} or Cr^{6+} or as a pair of two Cr ions for an aluminum−phosphorus pair. The latter seems to be more probable with respect to both the lack of an oxidant and the green color of the as-synthesized crystals. Both types of unstable Cr could easily leave the original positions during the thermal treatment/calcination and account for the observed amorphous material, clogging the pores and lowering the sorption, for the formation of meso- and macropores, and for the color effects due to multivalent Cr species (see below). The cause of the extremely high line intensity in XRD patterns cannot be deduced from the present results.

(27) Treacy, M. M. J.; Higgins, J. B.; von Ballmoos, R. *Collection of Simulated XRD Powder Patterns for Zeolites, Zeolites* (spec. edition); Elsevier: Amsterdam, 1996.

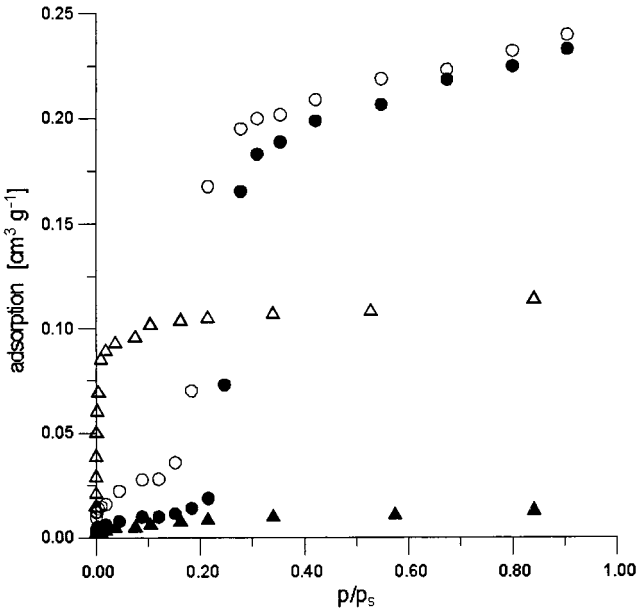

Figure 5. Adsorption isotherms for water (circles) and benzene (triangles) adsorbed on HS sample 5 (empty symbols) and LS sample 17 (full symbols).

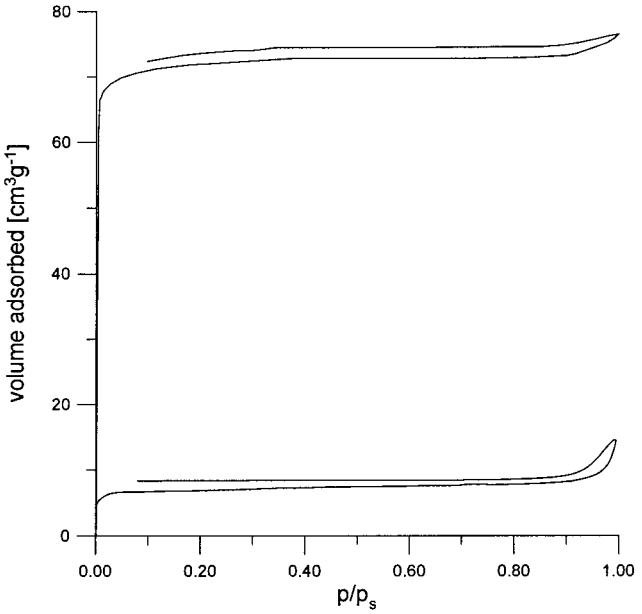

Figure 6. Adsorption isotherms for nitrogen adsorbed on HS sample 5 (upper curve) and LS sample 17 (bottom curve).

Sorption Properties. The sorption isotherms for adsorbates of various dimensions, shapes, dipole moments, and electron structures (H_2O, C_6H_6, N_2) supplied complex information about the accessibility of the pores. The synthesized products could be divided into two groups. Amorphous Al compounds yielded samples with a very low sorption capacity for benzene (Figure 5) and nitrogen[4,5] (Figure 6) while those synthesized from pseudoboehmite or pseudoboehmite-like Al compounds exhibited much higher sorption capacities[4,5] (Figures 5 and 6). The products synthesized with co-templating acetate ions showed a full sorption capacity, higher even than pure $AlPO_4$-5.[4] This was almost independent of the Cr content. Therefore, the materials will hereafter be referred to as LS for low and HS for high sorption capacity, respectively. In relation to N_2, the sorption

capacity of the HS samples decreased slightly with increasing Cr content.[4,5] This was accompanied by a slight decrease in pore volume with the content of Cr (Table 1).

The high sorption capacities for benzene and nitrogen proved open pore systems of the HS samples. A very weak hysteresis in the nitrogen isotherms[4,5] (Figure 6) indicated a low amount of mesopores or macropores. The strongly limited sorption capacities of the LS samples indicated that the pores were hardly accessible to either sorbate. The LS crystals had a clearly higher number of larger pores (Figure 6) and lower pore volumes (Table 1).

The relatively high sorption capacity of the samples synthesized using the classical method,[2] their elongated crystal morphology (no influence of Cr substitution), and a quite intense yellow color after calcination resulting from Cr^{5+} or Cr^{6+} (cf. sections *Colors* and *Morphology*) implied that Cr^{3+} was not incorporated into the framework, but mostly anchored to the external surface of the crystals. It was then not stabilized by the siting in the framework and could be oxidized.

The sorption isotherms of water (Figure 5) belonged to type IV or V (for extensive discussion see ref 5). The samples of both groups had an almost identical sorption capacity as pure $AlPO_4$-5.[4,5] The sorption capacity for water cannot be used as an indication of open or clogged pores as these small molecules can pass the 6-ring windows of the structure and penetrate the crystals "through the walls". However, the low-pressure step of the isotherms for water is sensitive to the content of heteroatoms substituted into the framework.[5] The HS samples showed a clear shift of the step to lower relative pressure with a growing content of Cr, which indicated that the Cr centers influence the sorption process. A stable position of the step for the LS samples revealed the lack of interactions between the adsorbent and water, that is, the absence of substituted chromium.[5]

Colors. All as-synthesized samples had a typical of Cr^{3+} compounds green color of the intensity following the Cr content. The colors also revealed differences between the two groups.

The HS samples (Table 1, No. 1−11) became intensively violet during calcination and, after cooling, they changed to yellow-green. The colors varied reversibly; that is, the samples could be turned to violet by heating them to over ≈550 K and back to yellow-green by cooling. The green color of as-synthesized HS CrAPO-5 is characteristic of the strongly preferred 6-fold coordination of Cr^{3+}. The violet color over ≈550 K may indicate occurrence of either the $[Cr^{III}O_{4/2}]^-$ or $[Cr^{III}O_{6/2}]^{3-}$ species, both of which can have that color.[28,29] However, the latter could not be substituted for $[AlO_{4/2}]^-$ for charge balance reasons. Thus, the only reasonable possibility is that the very unlikely tetrahedral coordination of Cr^{3+} in the framework is complemented by additional ligands located in the pores to form the distorted pseudo-octahedral one with its green color. Such a structure could be compatible with the observed color changes and the high stability of the substituted Cr^{3+} ions. Then, the color changes of the calcined HS crystals with temperature are concluded to correspond to de- and rehydration of the Cr centers.

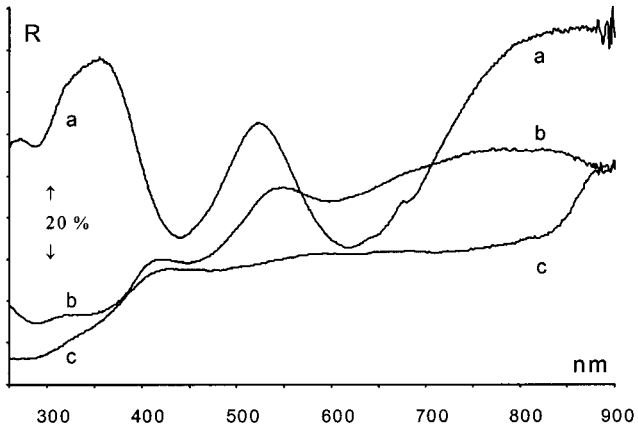

Figure 7. Diffuse reflectance UV−Vis spectra of HS CrAPO-5 (sample 9) with framework Cr: (a) as-prepared; (b) calcined, RT; (c) calcined, measured at elevated temperature.

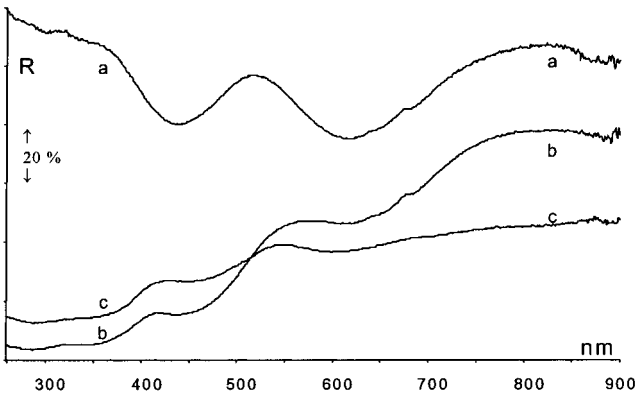

Figure 8. Diffuse reflectance UV−Vis spectra of LS CrAPO-5 (sample 15) with extra-framework Cr: (a) as-prepared; (b) calcined, RT; (c) calcined, measured at elevated temperature.

It remains an open question which ligands complement the coordination of Cr in the as-prepared crystals. However, the necessary presence of co-template(s) and the synergetic effects of Cr^{3+} ions and co-template on the morphology of the crystals strongly suggest that the co-template molecules play the role of additional ligands. The mass spectroscopy investigations failed to differentiate between the decomposition products of template and co-template.

The LS samples (Table 1, No. 15−18) turned greenish-gray to dark gray during calcination and retained that color independently of any thermal/vacuum treatment and its duration. The green color of the as-synthesized LS samples also reveals a 6-fold coordination of Cr. However, the gray color is indicative of multivalent Cr species.[28,29] Such clusters of a number of Cr atoms cannot be included in the framework and can only occur as extra-framework material clogging the pores. These Cr composites tend to stabilize under temperature treatment[28,29] and thus cannot be removed from the calcined crystals. The stable gray color of the calcined LS materials implies that Cr potentially incorporated during the synthesis is thermally unstable.

UV−Vis Spectroscopy. The diffuse reflectance UV−Vis spectra (Figures 7−9) show absorption bands of Cr without overlap of the framework bands. As the spectra have been measured for the large crystals, the curves

(28) Lever, A. B. P. *Inorganic Electronic Spectroscopy*; Elsevier: Amsterdam, 1984.
(29) Reinen, D. *Struct. Bond.* **1969**, *6*, 30.

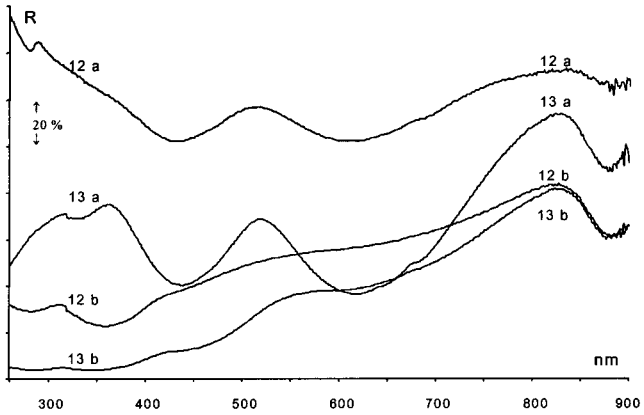

Figure 9. Diffuse reflectance UV−Vis spectra of comparative CrAPO-5 samples prepared from chromate salt (12) and using the classical method (13): (a) as-prepared; (b) calcined.

Table 2. Positions and Intensity of Absorption Bands of Chromium in Various Investigated CrAPO-5 Materials and in "Calcined" $Cr(NO_3)_3$ (Numbers of the Samples as in Table 1)

HS samples 1−11	LS samples 15−18	classical syntheses,[2,3] samples 13 and 14	from CrO_4^{2-}, sample 12	$Cr(NO_3)_3$
		As-Synthesized Samples		
292 w	301 vw	295 vw	275 w	not measured
			310 vw	
332 vw	335 w	331 vw	340 w	
440 vs	437 vs	437 s	430 vs	
473 sh	477 sh	472 sh	470 w	
620 vs	622 vs	621 vs	620 vs	
649 m	653 w-m	647 m	653 s	
686 m	687 w-m	685 m-s	691 m	
825 vw	820 vw	808 vw	823 vw	
		Calcined Samples		
283 vs	285 vs	287 vs	281 s	277 tr
350 m	347 s	350 vs	347 vs	348 vw
	365 vw		362 vs	
388 w		383 sh	382 m	378 s
449 m	445 m	444 m	435 m	435 sh
				458 vs
480 vw	490 vw			476 vs
606 sh	613 w	602 sh	604 w	600 vs
630 w−m	633 w-m	626 w	627 w	622 w
659 w−m	656 w-m	654 w	657 w	647 sh
691 w−m	687 w	690 w	691 tr	680 sh
820 vw	817 w	803 tr	833 vw	812 vw
		Spectra Measured at an Elevated Temperature		
295 vs	288 vs			
346 m−w	347 vs			
447 m	457 m	intensity symbols: vs, s, m, w, vw, sh, and tr		
490 w	476 m	denote very strong, strong, medium, weak,		
537 sh	511 w	very weak, shoulder, and traces, respectively		
	607 m			
641 m	631 m			
	660 vw			
810 vw	820 tr			

may contain contributions from specular reflection and can therefore be considered only qualitatively. For a better determination of absorption bands belonging to various Cr ions and coordination types, the spectra were deconvoluted using the Grams/32 program.[30] The resulting bands are listed in Table 2. This operation was performed taking into account the known absorption bands of chromium[8,9,28,29,31,32] listed in Table 3.

The spectra of the as-synthesized HS samples showed three characteristic bands at 292, 440, and 620 nm and sometimes very weak ones at ≈280 and 340 nm (Table 2, Figure 7). After calcination, the same bands were observed and the last one increased in intensity. At an elevated temperature (violet color) the bands at 440 and 620 nm almost vanished though absorption in this region remained relatively high, indicating a drastic broadening of all absorption bands present. The band at 295 nm showed a strong increase and thus became dominant. This band overlapped a weaker band located at about 346 nm (Table 2, Figure 7).

The as-synthesized LS samples showed the same three characteristic absorption bands at 301, 437, and 622 nm and a weaker one at 335 nm (Figure 8, Table 2). After calcination, all these bands broadened significantly and became much less pronounced and the strongest were located at 285 and 347 nm. This spectrum remained almost unchanged at an elevated temperature.

The spectra of as-synthesized comparative samples (Figure 9) prepared with use of the classical method[2] (Table 1, No. 13 and 14) and the chromate salt (12) showed no substantial differences in relation to the HS or LS samples. After calcination, the spectra of samples 12 and 13 were similar to those measured at elevated temperature for the HS and LS samples, respectively (Figures 7 and 8, Table 2). Their dominating bands were at about 285 and 340−360 nm.

A comparison of the results with literature data[8,9,28,29,31,32] (Table 3) shows two essential points. The positions of three bands characteristic of octahedral Cr^{3+} (Table 2) indicate lack of (i) Cr_2O_3 clusters and (ii) $[Cr(H_2O)_6]^{3+}$ complexes in the samples. The spectra also indicate that octahedral Cr^{3+} is the dominant form of chromium in all CrAPO-5 samples. The content of Cr(V) and/or Cr(VI) species is much lower than that of Cr^{3+}, as can be concluded from distinctly lower intensities of the corresponding absorption bands (Tables 2 and 3). The lack of a band at about 270 nm seems to indicate that Cr(V) is the main higher oxidized form. An increase in intensity of the absorption bands at 330−350 nm after calcination implies oxidation of a low fraction of chromium to Cr(VI) and/or Cr(V). Their contents are clearly higher in the LS than in the HS samples, as concluded from the presence of the bands at 365 and 606−613 nm.

The spectra measured at elevated temperature support this interpretation. A smoothing of the spectra of the HS samples and apparent vanishing of the main absorption bands of the octahedral complexes at 630 and 449 nm (Figure 7) is in agreement with the postulated 4-fold coordination of Cr under such conditions. In accordance with that, this spectrum is very similar to that (Figure 9) of the calcined sample synthesized from chromate salts (no octahedral Cr^{3+}). The LS samples do not reveal a strong difference in relation to the spectra of the calcined materials (Figure 8), that is, the two bands of octahedral Cr^{3+} species are clearly visible also at elevated temperature. Moreover, the strongest absorption bands are those at 288 and 347 nm, related to the absorption of both Cr(VI) and Cr(V). The spectrum is similar to that (Figure 9) of the calcined sample 13 (classical method with use of acetate anions). This

(30) Grams/32, Version 5.10, Galactic Industries Corp., 1998.
(31) Bakac, A.; Wang, W.-D. *Inorg. Chim. Acta* **2000**, *297*, 27 and refs 28−31 therein.
(32) Krumpolc, M.; DeBoer, B. G.; Roek, J. *J. Am. Chem. Soc.* **1978**, *100*, 145.

Table 3. Literature Data[8,9,29,30,32,33] on UV−Vis Spectroscopy of Chromium (L = Ligand, R = Organic Compound, C−T = Charge Transfer)

ion	species	coordination	transition	absorption (nm)
Cr^{2+}	CrL_6	octahedral O_h (to tetragonal D_4h)	$^5E_g \leftarrow {}^5T_{2g}$	675−825
Cr^{2+}	$[Cr(H_2O)_6]^{2+}$	octahedral O_h (to tetragonal D_4h)	$^5E_g \leftarrow {}^5T_{2g}$	715
Cr^{3+}	$[Cr(H_2O)_6]^{3+}$	(octahedral O_h to) tetragonal D_4h	$^4T_{1g}$ (P) $\leftarrow {}^4A_{2g}$	265
			$^4T_{1g}$ (F) $\leftarrow {}^4A_{2g}$	406
			$^4T_{2g} \leftarrow {}^4A_{2g}$	575
			$^2T_{2g}/{}^2E_g \leftarrow {}^4A_{2g}$	666
Cr^{3+}	$[CrL_6]^{3-}$	(octahedral O_h to) tetragonal D_4h	$^4T_{1g}$ (P) $\leftarrow {}^4A_{2g}$	290−310
			$^4T_{1g}$ (F) $\leftarrow {}^4A_{2g}$	307−440
			$^4T_{2g} \leftarrow {}^4A_{2g}$	375−671
			$^2T_{2g}/{}^2E_g \leftarrow {}^4A_{2g}$	640−760
Cr^{3+}	$[CrL_6]^{3+}$	(octahedral O_h to) tetragonal D_4h	$^4T_{1g}$ (P) $\leftarrow {}^4A_{2g}$	no data found
			$^4T_{1g}$ (F) $\leftarrow {}^4A_{2g}$	445 ± 20 or 350
			$^4T_{2g} \leftarrow {}^4A_{2g}$	630 ± 40 or 460
			$^2T_{2g}/{}^2E_g \leftarrow {}^4A_{2g}$	663 ± 8
Cr^{3+}	Cr_2O_3 clusters	octahedral O_h	d−d	as above, shifted to lower nm
Cr^{3+}	$[CrL'_4L''_2]^{n+}$ or $[CrL'_5L'']^{n+}$	tetragonal D_4h or pyramidal distorted C_4v	$^4T_{1g} \leftarrow {}^4A_{2g}$	370 ± 35
			$^4B_{2g} \leftarrow {}^4B_{1g}$	460 ± 15
			$^4E_g \leftarrow {}^4B_{1g}$	555 ± 45
Cr^{3+}	tungstochromic acid	tetrahedral T_d	d−d	625, 1205
Cr^{4+}	$Cr(OR)_4$	tetrahedral T_d	d−d	≈400, 649−676, ≈1100
Cr^{5+}	CrO_4^{3-}	tetrahedral T_d	$^2E \leftarrow {}^2T_2$	714−1052
			C−T O → Cr^{5+}	357−385
				585−625
Cr^{5+}	oxo species (chromyl)	pseudo-octahedral	C−T O → Cr^{5+}	399−476
				425−559
				724−801
Cr^{6+}	CrO_4^{2-}	tetrahedral T_d	C−T O → Cr^{6+}	245−285
				315−387
				≈450

sample is yellow due to dominating Cr(V)/Cr(VI) species but its spectrum also reveals weak bands of octahedral Cr^{3+}. All the above observations are in agreement with the gray color of the LS samples and support the presence of a mixture of all possible electron configurations and/or coordination states (multivalent Cr compounds).

Morphology of the Crystals. The crystal dimensions of all samples were distributed over relatively broad ranges (Table 1). Both the dimensions and the morphology of the crystals (SEM and light microscopy) depended on the gel composition, the use of co-templates, the preparation method, and the resulting substitution of Cr (Table 1, Figures 1 and 2). The whole group of the LS and reference samples had a morphology typical for the AFI structure type, that is, elongated, pencil-like hexagonal prisms with the aspect ratio l:d (length:width) up to ≈20 (Figure 1). Substitution of Cr in the HS samples resulted in shortening of the prisms along the hexagonal *c* axis usually to l:d of about 2.5−0.8 (Table 1, Figure 2). Acetate ions caused a further significant shortening of the crystals (Table 1) and l:d even lower than 0.1. In parallel, an enlargement of d was observed. These facts suggest a considerable synergetic effect of Cr and co-template on the morphology. Thus, we postulate that (i) the acetic acid molecules are included in the pore system of the crystals at Cr centers and (ii) Cr^{3+} substituting Al^{3+} in the framework strongly restrains the growth of the crystals along the *c* axis. Consequently, the CrAPO-5 crystals look like flat pellets (Figure 2). To our knowledge, this is the first time such flat crystals have been synthesized for an AFI structure type. The observed changes in the crystal morphology under substitution of Cr and introduction of acetate ions give good support for the above conclusions on Cr coordination.

Thermal Analysis. The loss of water from $AlPO_4$-5 (Figure 10A) occurred in two distinct steps at 323 and 427 K and equaled 3.8%. Partial removal of template (≈2%) occurred gradually up to ≈670 K. The remainder (≈4.2%) was removed at around 823 K. The HS CrAPO-5 samples lost water (≈4.7%) in one step up to ≈373 K and template (≈7.2%) also within one step with a maximum at ≈720 K (Figure 10B). The LS samples differed considerably (Figure 10C). Water was lost (≈4.3%) in two steps at ≈323 and 400 K while template was removed partially (≈1.5%) at ≈673 K and the main part (≈5%) was slowly burned off between 773 and 1273 K. The loss of mass due to template removal was equal to 6.7 ± 0.5% for all materials.

These results reflect large differences in the mechanisms of template removal between pure $AlPO_4$-5, HS CrAPO-5, and LS CrAPO-5 (Figure 10). The low- and high-temperature portions of template commonly removed during calcination correspond to a simple thermal decomposition or diffusion of some molecules and to the oxidation/burning out of those which cannot be removed, respectively. Such a behavior is observed for all three types of materials. The HS CrAPO-5 evolves the largest amount of template within the low-temperature step. This suggests either that the perfect structure of these crystals allows for fast removal of template or that Cr is distributed inhomogeneously, that is, more in the inside than in the external layer of the crystals. The insignificant removal of template from the LS samples indicates that the pores are closed as, if this were not the case, partial removal from the external layer of the crystals could be observed. The oxidation of template occurs at the highest temperature and suggests an extremely slow and difficult removal of the resulting products up to 1270 K. All these effects were accompanied by even better-defined changes in the DSC

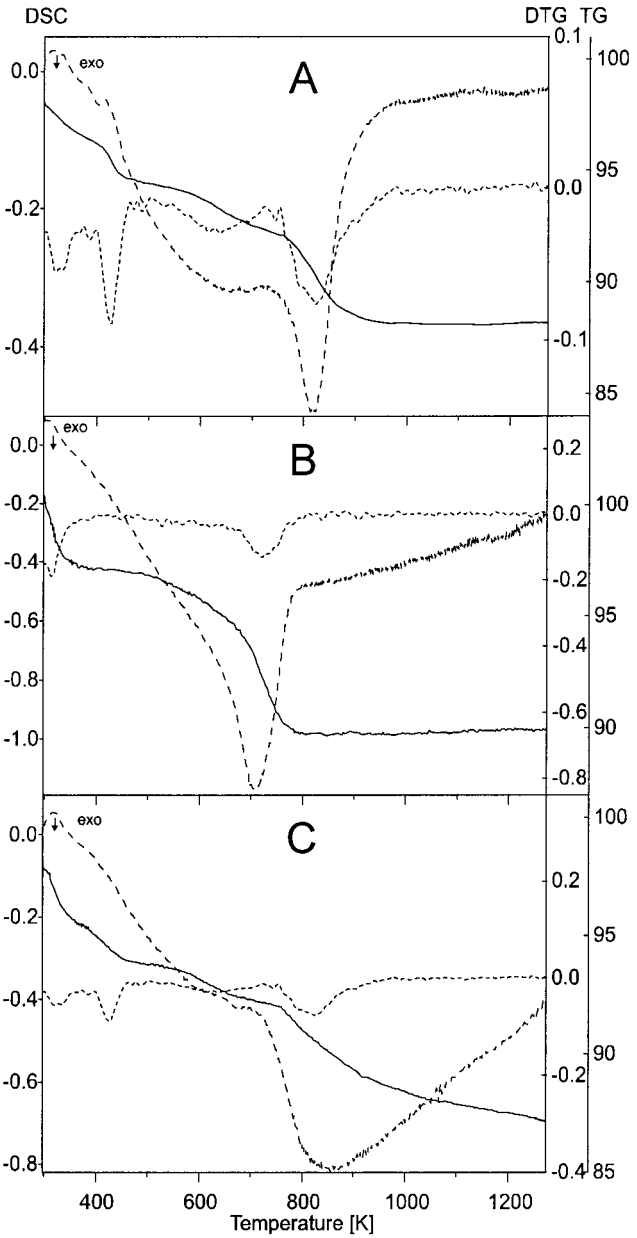

Figure 10. TG, DTG, and DSC curves (solid, dotted, and dashed lines, respectively) for $AlPO_4$-5 (A), HS CrAPO-5 sample 3 (B), and LS CrAPO-5 sample 18 (C).

curves, reflecting endothermal loss of water and exothermal burning of the template(s).

Thermal analysis was also used to examine the reversible (de)hydration of the calcined HS samples (Figure 11). A sharp loss of mass at about 335 K was followed by a further slight one (0.8%), which began at about 423 K and reached a maximum at 573−673 K. This slight loss of mass and accompanying thermal effect (Figure 11) correspond to the occurrence of the violet color of Cr, that is, to the removal of water bonded to the Cr centers. In fact, the recalculation reveals that 0.8% corresponds exactly to two water molecules per one Cr (sample 5, Table 1).

Stability of Cr. The tests of leaching the CrAPO-5 materials with acetic acid solutions did not indicate any loss of Cr from either the HS or the LS samples. No loss of Cr was observed in repeatedly done calcination and cooling cycles. Also, no ion-exchange properties were

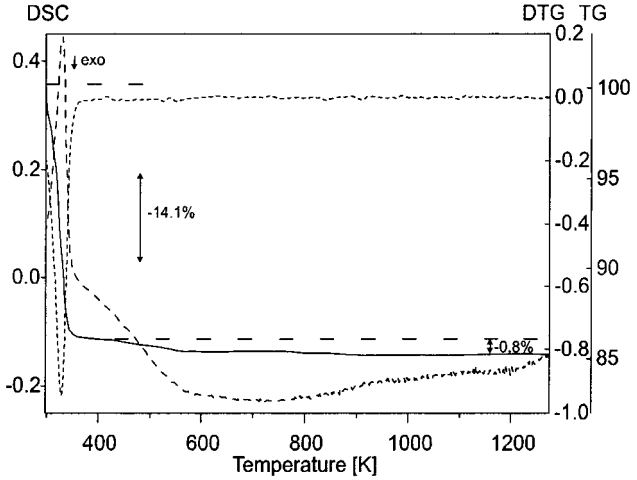

Figure 11. TG, DTG, and DSC curves (solid, dotted, and dashed lines, respectively) for calcined HS CrAPO-5 (sample 5).

found for the HS or LS samples. The negative results of these tests indicate in accordance with the other evidence that the Cr^{3+} ions are located in the HS samples in chemically and thermally stable framework positions and are substituted for Al^{3+}, which results in no framework charge. The bulky multivalent Cr species of the LS samples are blocked in the pores due to steric hindrances.

EPR Spectroscopy. A more detailed discussion of the extensive EPR results is given separately.[20] Two broad EPR signals observed for the as-synthesized samples at about $g_1 = 5.2$ and $g_2 = 2.0$ (cf. ref 20) have been assigned to components of the anisotropic line of Cr^{3+} in a distorted octahedral coordination.[17,18,20] Apart from differences in intensities, the lines did not differ between the samples. The axially symmetric line observed for the calcined samples in the region around $g = 2$ has been assigned to Cr^{5+} in tetrahedral coordination.[17,18,20] By line-shape simulation, the values $g_\perp = 1.972$ and $g_{||} = 1.961$ were derived.[20] The spectra of the LS samples 16 and 17 exhibited an additional isotropic line at $g = 2.00$ caused by coke radicals.[33]

NMR Spectroscopy. The ^{27}Al MAS NMR spectra of the as-synthesized samples are not shown as they resembled those usually obtained[34−36] for as-synthesized $AlPO_4$-5 or SAPO-5 with the dominating line of the tetrahedrally coordinated Al atoms at ≈36 ppm. It could be expected as substitution of Cr for Al should cause no changes around the Al atoms. A broad line at −10 ppm and a shoulder at about 15 ppm were assigned to the octahedrally and pentacoordinated Al atoms very often present in as-synthesized aluminophosphate-based molecular sieves, respectively.[34] The ^{31}P MAS NMR spectra (also not shown due to their typical form) exhibited asymmetric broad (fwhh = 12 ppm) lines with a maximum at about −29 ppm.

After calcination, symmetric or almost symmetric resonance lines at (−30.2 ± 0.1) ppm and (32.5 ± 0.2) ppm with significantly reduced line widths to fwhh = 4

(33) Lange, J.-P.; Gutsze, A.; Karge, H. G. *J. Catal.* **1988**, *114*, 136.
(34) Blackwell, C. S.; Patton, R. L. *J. Phys. Chem.* **1988**, *92*, 3965.
(35) Goepper, M.; Guth, F.; Delmotte, L.; Guth, J. L.; Kessler, H. *Stud. Surf. Sci. Catal.* **1989**, *49*, 857.
(36) Zibrowius, B.; Löffler, E.; Finger, G.; Sonntag, E.; Hunger M.; Kornatowski, J. *Stud. Surf. Sci. Catal.* **1991**, *65*, 537.

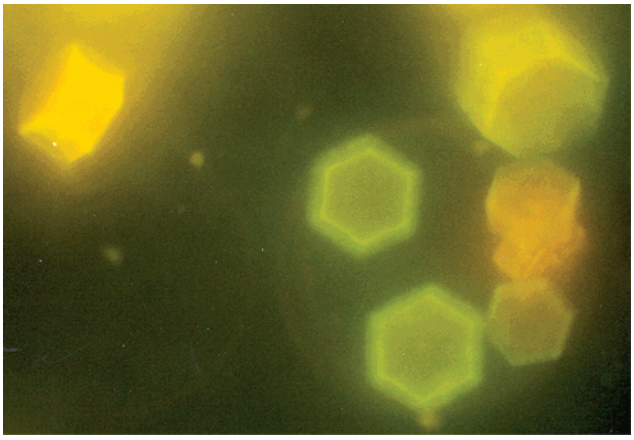

Figure 12. Fluorescence-microscopic picture of HS CrAPO-5 crystals loaded with azobenzene.

and 10 ppm were observed in the ^{31}P and ^{27}Al MAS NMR spectra, respectively. These results also corresponded to those for $AlPO_4$-5 and SAPO-5.[35−37] (When comparing the ^{27}Al NMR line positions in spectra recorded at a different field strength, one has to take into account the field dependence of the second-order quadrupolar shift.) In the case of sample 15, the ^{31}P resonance line was significantly broader (fwhh = 6 ppm) and the maximum was shifted to −29.4 ppm. No additional line or shoulder was observed for any of the calcined samples.

The lack of additional resonance lines in the ^{31}P MAS NMR spectra does not disprove the framework substitution of Cr. The incorporation of paramagnetic Cr^{3+} into the framework could have a similar effect as the incorporation of Co into various aluminophosphates.[38] In this case, some of the P atoms become effectively undetectable by conventional NMR techniques. The application of the spin−echo mapping (SEM) technique would be necessary to record the very broad and heavily shifted resonance lines.[38]

Fluorescence Investigations. The accessibility of the pore system was also probed by adsorption of dyes. Although the dyes can fit into the channels, disturbances inside the pores can often block them or hinder the diffusion. The pores of the HS crystals were inaccessible to the polar *p*-nitroaniline (pNA) but easily accessible to the nonpolar azobenzene. After a slow calcination process, the single crystals of CrAPO-5 were loaded with azobenzene, which was adsorbed homogeneously and in a high concentration. They showed (Figure 12) an orange color and a clearly visible, inhomogeneously distributed, green fluorescence in the range of 450−550 nm. The unique platelike morphology of the crystals enabled easy observation in different directions. Under a microscope, it was evident that the fluorescence originates mainly from the side faces of the hexagonal prisms and is independent of crystal size.

A similar fluorescence with a maximum in the green region of the spectrum has already been described by Lei et al.[39] and assigned to protonated azobenzene Without protonation, the fluorescence of azobenzene is strongly quenched. Therefore, the observed fluorescence suggests that protonation of azobenzene also occurs in the CrAPO-5 crystals. This could occur at very low concentrations of defects located only near the side faces of the crystals. This suggests the influence of disturbances in the homogeneous distribution of $AlO_{4/2}^-$ and $PO_{4/2}^+$ tetrahedra due to the Cr centers and may agree with the Cr distribution implied by thermal analysis. Another possibility is the effect of the atypical coordination of Cr on sorption of dyes.[5] Such "inhomogeneous regions" around substituted Cr might interact with the polar pNA molecules strongly enough to hinder the diffusion and loading. Thus, the azobenzene fluorescence could possibly be used as a probe method for site disturbances. The phenomenon is under further investigation.

Conclusions

The CrAPO-5 crystals of high sorption capacities and with a high content of stably substituted Cr can be synthesized using a procedure based on the new co-templating effect. The necessary conditions are as follows: (i) a pseudoboehmite(-like) Al compound and (ii) use of a co-template, for example, acetate ions or other aliphatic acids.[22] Without the co-template, lower amounts of Cr are incorporated. Without the appropriate Al source, the crystals of low sorption capacities (N_2 volume below 15 cm^3/g) are formed, the pores of which are clogged with extra-framework Cr species. The Cr^{3+} ions are substituted into the framework of the highly sorbing (N_2 volume over 70 cm^3/g) crystals for Al mainly in the form of the $CrO_{4/2}^-$ units which are complemented by two ligands located in the pores to form the distorted octahedral (tetragonal) coordination. These ligands are H_2O molecules after calcination and probably co-template molecules in the as-synthesized crystals. The CrAPO-5 crystals of high sorption capacities reveal a high chemical and thermal stability as well as no additional framework charge compared to $AlPO_4$-5. The Cr species cause a green color, which changes to intensive violet under heating above ≈550 K because of the removal of the two additional H_2O ligands and transition to 4-fold coordination. That is quantitatively confirmed by thermal analysis of the calcined samples. The violet color of the dehydrated samples of high sorption capacities is likely indicative of isomorphous substitution of Cr^{3+}. Both the substitution of Cr and the use of co-template(s) strongly affect the morphology of the crystals, that is, cause their shortening along the *c* axis. With the help of the synergetic effect of both factors, the crystals can be grown as flat hexagonal pellets. The co-template(s) exert a favorable buffering influence and control the synthesis by controlling the pH value of the reaction gel. The co-templated synthesis gives rise to a reaction mechanism that results in very high crystallinity, perfect morphology, and high sorption capacities of the products.

Acknowledgment. The work was partially supported by the Deutsche Forschungsgemeinschaft (DFG) and the Polish Committee for Scientific Research (KBN). Thanks are due to Prof. P. Kita (UMK, Torun, Poland) for the helpful discussions on the UV−Vis spectra of chromium.

CM0011864

(37) Zibrowius, B.; Löffler E.; Hunger, M. *Zeolites* **1992**, *12*, 167.
(38) Canesson, L.; Boudeville, Y.; Tuel, A. *J. Am. Chem. Soc.* **1997**, *119*, 10754.
(39) Lei, Z.; Vaidyalingam, A.; Dutta, P. K. *J. Phys. Chem. B* **1998**, *102*, 8557.